Ice-cored moraine degradation mapped and quantified using an unmanned aerial vehicle: a case study from a polythermal glacier in Svalbard

Tonkin, T.N[a,*]., Midgley, N.G[a]., Cook, S.J[b] and Graham, D.J[c]

[a] School of Animal, Rural and Environmental Sciences, Nottingham Trent University, Brackenhurst Campus, Southwell, Nottinghamshire, UK

[b] School of Science and the Environment, Manchester Metropolitan University, Manchester, UK

[c] Polar and Alpine Research Centre, Department of Geography, Loughborough University, Leicestershire, UK

[*] Corresponding Author: + 44 115 848 5257 toby.tonkin@ntu.ac.uk

Keywords

Structure-from-Motion, deglaciation, geomorphologic change detection, Austre Lovénbreen

Highlights

- SfM photogrammetry used to produce topographic data from archive aerial imagery and UAV derived aerial imagery
- Datasets from 2003 and 2014 were compared to report on the de-icing of a lateral-frontal ice-cored moraine
- The moraine appears to be de-icing predominantly via down-wastage affording the moraine a higher degree of stability
- UAVs and SfM are shown to be useful tools for monitoring environmental change

Abstract

Ice-cored lateral-frontal moraines are common at the margins of receding high-Arctic valley glaciers, but the preservation potential of these features within the landform record is unclear. Recent climatic amelioration provides an opportunity to study the morphological evolution of these landforms as they de-ice. This is important because high-Arctic glacial landsystems have been used as analogues for formerly glaciated areas in the mid-latitudes. This study uses SfM (Structure-from-Motion) photogrammetry and a combination of archive aerial and UAV (unmanned aerial vehicle) derived imagery to investigate the degradation of an ice-cored lateral-frontal moraine at Austre Lovénbreen, Svalbard. Across the study area as a whole, over an 11-year period, the average depth of surface lowering was -1.75 ± 0.89 m. The frontal sections of the moraine showed low or undetectable rates of change. Spatially variable rates of surface lowering are associated

with differences in the quantity of buried ice within the structure of the moraine. Morphological change was dominated by surface lowering, with limited field evidence of degradation via back-wastage. This permits the moraine a greater degree of stability than observed at other sites in Svalbard. It is unclear whether the end point will be a fully stabilised ice-cored moraine, in equilibrium with its environment, or an ice-free lateral-frontal moraine complex. Controls on geomorphological change (e.g. topography and climate) and the preservation potential of the lateral-frontal moraine are discussed. The methods used by this research also demonstrate the potential value of SfM photogrammetry and unmanned aerial vehicles for monitoring environmental change and are likely to have wider applications in other geoscientific sub-disciplines.

1. Introduction

In Svalbard, the Neoglacial maxima of land-terminating glaciers are typically demarcated by large lateral-frontal moraine complexes (e.g. Bennett et al., 1996; Lyså and Lønne, 2001; Glasser and Hambrey, 2003; Lønne and Lyså, 2005; Lukas et al. 2005; Ewertowski et al. 2012; Midgley et al., 2013). The persistence of relict ice in such moraines is testament to extensive permafrost conditions at the margins of these glaciers (Etzelmüller and Hagen, 2005). However, climatic amelioration and deglaciation are contributing to the de-icing of ice-cored landforms (e.g. Etzelmüller, 2000). Whilst the dynamics of de-icing have been studied (e.g. Schomacker 2008; Irvine-Fynn et al., 2011; Bennett and Evans, 2012), the

resulting preservation potential of these landforms in the geomorphological record is unclear (Bennett et al., 2000; Evans, 2009). Knowledge regarding the formation and preservation of glacial landforms is of interest due to the potential for contemporary glacial environments to be used as analogues for formerly glaciated environments in the mid-latitudes (e.g. Hambrey et al., 1997; Graham and Midgley, 2000; Benn and Lukas, 2006; Graham and Hambrey, 2007; Midgley et al., 2007). Moraines are important palaeoenvironmental proxies (Kirkbride and Winkler, 2012), and understanding their genesis and potential for preservation in the geomorphological record is an essential prerequisite for robust interpretations of relict moraine assemblages. Rates of wastage on ice-cored moraines are understood to be principally driven by surface processes and topography, rather than climatic conditions (Schomacker, 2008). In the high-Arctic glacial environment, some ice-cored moraines are reported to be unstable and somewhat transient geomorphological features, with ultimately low preservation potential (Bennett et al., 2000; Lukas et al., 2005). Conversely, where debris cover is sufficiently thick, it has been reported that ice-cored moraine may stabilise, undergoing limited or negligible rates of transformation (Ewertowski, 2014; Ewertowski and Tomczyk, 2015).

Geoscientists now have access to a range of new technologies for monitoring the temporal evolution of geomorphological systems. Specifically, automated photogrammetric techniques such as SfM are an excellent tool for conducting high-resolution topographic surveys (James

and Robson, 2012; Westoby et al., 2012; Carrivick et al., 2013; Fonstad et al., 2013). SfM photogrammetry has also been integrated with small format, low-level aerial imagery acquired from small UAVs (e.g. Lucieer et al., 2013; Tonkin et al., 2014; Ryan et al., 2015; Smith and Vericat, 2015; Clapyut et al., 2015; Rippin et al., 2015). Here, SfM photogrammetry was used to document the evolution of an ice-cored lateral-frontal moraine over an 11-year study period, based on images obtained with a UAV in 2014 and archive images from a piloted aircraft in 2003. The principal aims of this study were to: (1) report on the use of SfM for Digital Elevation Model (DEM) production from both archive and small-format low-level aerial imagery for the purpose of assessing environmental change in the high-Arctic; (2) investigate landform evolution at the margins of a high-Arctic glacier; and (3) discuss the geomorphological evolution of ice-cored moraine in relation to landform stability and preservation potential.

2. Study site

Austre Lovénbreen is a *c.* 5 km long valley glacier located on Brøggerhalvøya, Spitsbergen, Svalbard (78°53′12″N 12°08′50″E; Fig. 1). The thermal regime of the glacier was polythermal in 2010 based on our interpretation of GPR (ground-penetrating radar) profiles presented by Saintenoy et al. (2012); the extent of temperate ice appeared to be exceptionally spatially limited, with the glacier being almost entirely cold-based. Austre Lovénbreen has a strong negative mass balance according to Friedt et al. (2012), who reported a mean ablation rate of 0.43 m a^{-1}

between 1962 and 1995, which increased to 0.70 m a^{-1} for the 1995–2009 period.

The glacier is surrounded by mountainous terrain with peaks ranging from 583 m a.s.l. (Slattofjellet) to 879 m a.s.l. (Nobilefjellet) at the head of the basin. Surge-type glacier behaviour is widely reported in Svalbard (e.g. Jiskoot et al., 2000). The potential for surge-type behaviour at adjacent glaciers on Brøggerhalvøya has been discussed (e.g. Hansen, 2003; Glasser et al., 2004; Hambrey et al., 2005) and disputed (e.g. Jiskoot et al., 2000; King et al., 2008). However, Midgley et al. (2013) presented evidence that Austre Lovénbreen may have surged close to or at its Neoglacial maximum position based upon the interpretation of oblique Norsk Polarinstitutt (NPI) aerial imagery from 1936.

The character of the glacier forefield was documented by Hambrey et al. (1997), with additional field observations reported by Graham (2002). The glacier forefield is characterised by a large arcuate lateral-frontal moraine, which is breached at two locations by the main contemporary glaciofluvial outlets. The lateral-frontal moraine demarcates the Neoglacial limit based upon interpretation of ground-level imagery from 1907 (Isachsen, 1912) and oblique Norsk Polarinstitutt (NPI) aerial images from 1936 (Fig. 6 in Midgley et al., 2013). The glacier has receded *c*. 1 km from this position. Within the Neoglacial limit, surface hummocks (‘hummocky moraine’) are identified. Fluted diamicton plains and lineated accumulations of supraglacial debris (e.g. Hambrey et al., 1997) have developed as Austre

Lovénbreen receded from its Neoglacial position. More recently, the structural characteristics of the lateral-frontal moraine around the western margin of the forefield were investigated by Midgley et al. (2013) using GPR. This research found that in lateral sections an ice-core constitutes a significant component of the landform, in contrast to the frontal sections where the occurrence of buried ice is limited. This paper maintains the focus on the western margin of the forefield, providing surface morphological data to complement the subsurface data presented by Midgley et al. (2013).

3. Materials and methods

3.1. Data acquisition

Five images from 2003 were obtained from the UK Natural Environment Research Council (NERC) Airborne Research and Survey Facility (ARSF) for DEM production. These images were collected on August 9th 2003 using a metric camera mounted in a Dornier 228 aircraft, and the contact prints scanned to give an approximate ground resolution of 0.2 m per pixel. In 2014, 10 UAV sorties were flown over a two-day survey period (15th and 16th July 2014). The total area covered by this survey is *c*. 676,000 m^2. A DJI S800 multi-rotor UAV equipped with an 18 MP Canon EOS-M consumer-grade digital camera was used for image acquisition. The UAV was flown at approximately 100 m above ground level, giving a ground resolution of 0.02 m per pixel. A total of 1856 images from this survey were used for DEM production. Further details on this survey setup and validation against a total station derived survey were documented by Tonkin et al. (2014).

Ground control points were surveyed using a Leica 1200 dGPS and post-processed using RiNEX data obtained from the EUREF Permanent Network station at Ny-Ålesund (http://www.epncb.oma.be/_networkdata/). For the 2003 imagery, three ground control points were used to georeference the point cloud, and to project it to the UTM 33N coordinate system (Fig. 2). These were the tops of boulders which were visible on the original scanned contact prints, and also readily identified in the field. As the parts of the glacier forefield are likely to be geomorphologically unstable (e.g. Irvine-Fynn et al., 2011), where possible control points were located outside of the Neoglacial moraine. The 2014 imagery was georeferenced using 27 ground control-points consisting of A3 sized paper targets placed on snow-free areas of the moraine (Fig. 2).

3.2. DEM generation

DEM generation was conducted in Agisoft Photoscan (v. 1.1.5), a commercial SfM software package. A total of 2035 tie-points were automatically identified on the five images from 2003. For the 2014 imagery, processing was split between two ‘chunks’ that were merged to form a single DEM of the lateral-frontal moraine. Photoscan identified a total of 5,660,015 tie points from the 1856 images with the resulting DEM produced from a dense point cloud of 106,484,427 points. Both SfM DEMs were produced at 0.5 m per pixel resolution to facilitate comparison between them. On the 2003 DEM, moraine distal slopes were subject to

182 shading, resulting in excessively interpolated elevation data. Zones
183 identified with these issues were removed prior to analysis.

184 *3.3. Evaluation of DEM quality*

185 LiDAR data, obtained concurrently with the 2003 aerial imagery were used
186 to independently validate the 2003 DEM. DEM elevations were compared
187 with LiDAR spot heights distributed across the area of interest, giving a
188 vertical *RMSE* (root mean square error) value of 0.888 m (n = 768,296; σ
189 = 0.812 m). The residuals appear to be spatially distributed and increase
190 in areas subject to poor ground control, thus the 2003 SfM DEM may
191 represent an overestimate of the surface topography. However, it is worth
192 noting that the LiDAR data are not error free – the heights have been shown
193 to have an *RMSE* value of < 0.15 m in the area of interest (Arnold et al.,
194 2006) – but as the two datasets were obtained simultaneously their
195 comparison provides an independent means of estimating DEM error.

196 Two interrelated issues are likely to account for the vertical *RMSE* value in
197 this model: (1) the use of relatively low resolution of the imagery on which
198 the DEM is based; and (2) the identification of appropriate 'stable' features
199 to use as ground-control. The first issue reduces the accuracy with which
200 the location of control points can be identified in the imagery. In practice,
201 it is estimated that the identification of control points in the images
202 introduced an error of approximately 1 m. The low resolution also meant
203 that only a small number of large boulders were visible in the imagery,
204 limiting the number of sites available for use as ground control points. This

205 issue was confounded by the need to locate control points on features that
206 were unlikely to have moved during the 11 years between image capture
207 and the field survey. Use of existing ‘stable’ features for ground control is
208 a limitation of studies that use photogrammetric methods to produce DEMs
209 of changing geomorphological systems (e.g. Schiefer and Gilbert, 2007;
210 Staines et al., 2015), and means it is rarely possible to achieve an optimal
211 distribution of GCPs (ground control points). In this study only three
212 suitable boulders were identified for use as GCPs, which is highly likely to
213 have contributed to an increase in errors (e.g. Clapuyt et al., 2015).

214 For the 2014 DEM, errors were calculated for 12 dGPS surveyed check
215 points, which were paper targets visible in the imagery, additional to the
216 27 control points used to generate the model (Fig. 2). Sub-decimetre
217 vertical errors were obtained for these points (*RMSE* = 0.048 m; *n* = 12).
218 These error estimates give us confidence that the DEM provides an
219 excellent representation of the moraine morphology. For additional
220 validation, randomly generated spot heights (*n* = 4370) from more
221 geomorphologically ‘stable’ areas (e.g. Staines et al., 2015) outside the
222 Neoglacial limit on the 2003 and 2014 SfM DEMs were compared. Values
223 from these areas show lower error levels (*RMSE* = 0.374 m; σ = 0.274 m),
224 giving confidence in the validity of the two SfM DEMs.

225 *3.4. DEM differencing and minimum levels of detection*

226 DEM differencing – subtracting spatially coincident raster grid cells from
227 each other – was used to assess the amount of morphological change

between 2003 and 2014. DEM differencing was conducted using the GCD (Geomorphologic Change Detection, ver. 6) plugin of Wheaton et al. (2010) in ArcGIS 10.2.1. The GCD plugin allows for robust error assessment through the use of 'minimum levels of detection' (minLOD). This approach minimises the likelihood of making spurious interpretations of apparent morphological differences that are actually associated with uncertainty in the data. Minimum levels of detection were calculated using a propagated error value derived from error assessments undertaken on both topographic surfaces (e.g. Braslington et al., 2003). The technique assumes error within topographic datasets are spatially uniform, and discards changes below this threshold. For the 2003–2014 time period, vertical differences under 0.89 m were regarded as potentially erroneous, and therefore disregarded for the purposes of assessing morphological change. The majority of this uncertainty results from errors in the 2003 DEM. Three zones (Z_1, Z_2 and Z_3) were clipped from the differenced DEM and used to report on spatial variations in geomorphological change across the landform (Fig. 3A).

3.5. Feature mapping

The relative abundance of features indicative of ice-cored moraine degradation were mapped and used to validate the reported rates of surface change derived from the DEM differencing. Features were identified and mapped from ultra-high resolution (2 cm per pixel) orthorectified imagery produced from the 2014 survey data. These observations were

supplemented by field observations collected simultaneously to the acquisition of the 2014 topographic data. The study area was split into 50 x 50 m grid squares (n = 234) to allow the relative abundance of geomorphological features indicative of surface change to be qualitatively assessed across the study area. As the precise mode of formation for micro-topographic features indicating landform degradation was unclear, we adopted the non-genetic classification of 'surface linear undulations' to refer to features developed by the slumping and/or the extensional surface fracturing of materials in response to surface lowering (e.g. Kjær and Krüger, 2001; Krüger et al., 2010). The location of a large-scale arcuate edge and a linear back-wasting edge were also mapped.

4. Results

4.1. DEM differencing

A total area of 461,429 m^2 was assessed for surface elevation change (Fig. 3A). The lateral-frontal moraine shows a level of geomorphological stability, with change detected on 52% (238,476 m^2) of the study area. Ninety-six percent of the area where change was detected was associated with surface lowering. The total volume difference for the study area was −377,490 ± 201,292 m^3.

A clear spatial trend characterises the pattern of morphological change. The lateral up-glacier sections are subject to higher rates of surface lowering. Average surface change in Z_1 was −2.56 m for the study period. Nearly all grid cells in this area were observed outside the minimum level of detection.

Z_2 and Z_3, which are located in more frontal positions show diminishing rates of detectable change (92.3% and 19.9% of each study area, respectively) and lower rates of average net surface change (−1.49 and −0.52 m, respectively). Profiles 1, 2 and 3 in Fig. 4 also demonstrate reduced surface lowering in frontal positions. On profile 1, surface lowering is clearly evident on the moraine ridge crest, and less extensively on the ice-proximal and distal slopes. Profiles 2 and 3 show limited geomorphological change with a significant proportion of change falling close to or below the minLOD (Fig. 4). Detectable change on the outwash-plain was limited. Areas of deposition principally occur on moraine distal slopes and in proximity to glaciofluvial drainage systems. Areas that have experienced deposition across the study averaged a depth of 1.42 ± 0.89 m. However the deposition was extremely spatially and volumetrically limited, only accounting for the movement of 17,952 ± 11,267 m^3 of material (4% of the area of detectable change) opposed to 413,394 ± 212,243 m^3 of change associated with surface lowering across the study area (Fig. 3B). It should be noted that in 2014 *c.* 11% of the study area was covered by exceptionally late-lying snow, which was typically located in sheltered areas between pronounced ridges and contributes to the lowering of estimates of surface change over the study period.

4.2. Geomorphological evidence of surface change

The occurrence of features indicative of surface evolution were mapped to validate the derived rates of surface change (Fig. 5). Mapped surface

297 features indicative of surface change were identified in the lateral-zone of
298 the moraine complex; however, the features were less readily identified on
299 the frontal zone of the landform. Out of the 234 survey grid squares
300 assessed, 150 (64%) had no observable evidence of surface evolution. One
301 ice-free actively back-wasting slope was located on the frontal zone of the
302 analysis area adjacent to the western fluvial outlet channel which dissects
303 the Neoglacial lateral-frontal moraine. An additional inactive arcuate back-
304 wasting edge was identified in the lateral zone of the landform (Fig. 5). The
305 spatial occurrence of evidence associated with surface change gives us
306 confidence in the results of the DEM differencing.

307 **5. Discussion**

308 *5.1. Comparisons with other glaciers*

309 A range of studies provide rates of ice-cored landform degradation. Here,
310 rates of landform degradation appear to be limited in comparison to some
311 sites in Svalbard and elsewhere. For example, Irvine-Fynn et al. (2011)
312 report a moraine surface lowering rate of −0.65 ± 0.2 m a^{-1} at neighbouring
313 Midtre Lovénbreen between 2003 and 2005. Longer-term changes (1984–
314 2004) at Holmstrombreen (Svalbard) were reported to have occurred at a
315 rate of −0.9 m a^{-1} (Schomacker and Kjær, 2008). Rates of surface lowering
316 in temperate Icelandic glacial environments are variable (between −0.015
317 and -1.4 m a^{-1}; e.g. Krüger and Kjær, 2000; Schomacker and Kjær, 2007;
318 Bennett and Evans, 2012). On average, surface lowering for the entire
319 study area was considerably lower at −0.16 m a^{-1} than reported at some

sites in Svalbard. It should be noted that the rate of change may not have remained consistent throughout the study period with moraines known to be subject to short-term changes over consecutive years (e.g. Ewertowski and Tomczyk, 2015). Even in areas with the highest levels of surface lowering (e.g. Z_1), only modest rates of average surface change per year were detected (–0.23 m a^{-1}), which at worst, can be considered an overestimate of surface change, for example, due to errors on the 2003 SfM DEM. These results are similar to the findings of Ewertowski and Tomczyk (2015) who report on surface lowering at the margins of Ebbabreen and Ragnarbreen in Petuniabukta. Here, whilst areas of back-wasting ice were quantified to undergo changes of up to 1.8 m a^{-1}, lower levels of transformation (e.g. below 0.3 m a^{-1}), were quantified, highlighting the relative stability of some ice-cored moraine in Svalbard. Similarly, at Austre Lovénbreen, just over half of the study area (52%) was below the minimum level of detection implying no or exceptionally limited geomorphological change between 2003 and 2014.

5.2. Moraine preservation potential

Moraines in the high-Arctic glacial environment are understood to be highly vulnerable to thermo-erosion and mass movement facilitated by fluvial undercutting. This can result in high rates of landform transformation (Ewertowski and Tomczyk, 2015). The evidence presented here indicates that such surface processes are less important with regard to the transformation of the lateral-frontal moraine at Austre Lovénbreen. A

surface excavation in proximity to Z_1 showed that the debris mantle was surprisingly thick at 1.6 m. At this site, and potentially others, whilst rates of moraine surface lowering may be rather high, a relatively thick and evenly distributed debris-layers can permit the relative stabilisation of ice-cored moraine where the coupling of slope and fluvial processes (e.g. Etzelmüller et al., 2000) exert less influence on moraine transformation. This is largely due to the less topographically confined setting of the lateral-frontal complex at Austre Lovénbreen, which results in the glaciofluvial system being well separated from the moraine. The result is a low level of transformational activity, which principally occurs via down-wasting (e.g. Fig. 5). An implication of this study is that the ice-cored moraines formed at Austre Lovénbreen, and potentially other valley glaciers in Svalbard (e.g. the recent results of Ewertowski and Tomczyk, 2015), may have higher preservation potential than previously recognised as insulating debris is not reworked and remains *in situ*.

During the final stage of moraine development, two end-points are envisaged: (1) a fully stabilised ice-cored moraine, which is in equilibrium with its environment; or (2) an ice-free lateral-frontal moraine complex (Fig. 6). The first scenario requires a thick debris mantle to develop that exceeds the permafrost active layer allowing buried-ice to be a persistent landscape feature. It is unclear whether the first scenario is plausible. Ice-cored 'controlled' moraines are understood to be poorly preserved in the geomorphological record (Evans, 2009). Buried-ice up to 200 years of age has been documented in moraines at the margins of temperate Icelandic

367 glaciers (e.g. Everest and Bradwell, 2003). Examples of where the
368 preservation of buried-ice has been permitted on longer timescales include
369 formerly glaciated continental settings (e.g. Ingólfsson and Lokrantz, 2003;
370 Murton et al., 2005), and cold deserts where buried-ice is suggested to
371 have existed for several millennia under permafrost conditions (Sugden et
372 al., 1995; Schäfer et al. 2000). Waller et al. (2012) highlighted that the
373 preservation of buried-ice may be permitted on geological timescales if it
374 is located at depths unaffected by seasonal thaw. However, the high-Arctic
375 glacial environment in Svalbard is known for its highly unstable ice-cored
376 moraine, and rapidly progressing mass wasting processes (Bennett et al.,
377 2000; Schomacker, 2008; Irvine-Fynn et al., 2011; Ewertowski and
378 Tomczyk, 2015). Schomacker (2008) showed that climatic variables are
379 only weakly correlated with rates of ice-cored back-wastage occurring at
380 14 different glaciers; the implication being that surface processes and
381 topography are more important determinates of moraine disintegration.
382 However, this result may not hold at Austre Lovénbreen, where very limited
383 evidence of back-wasting was observed in the field by the authors in 1999,
384 2009 and 2014 (e.g. Fig. 5).

385 Alternatively, the second end-point requires complete de-icing of the
386 moraine, where the active layer may continue to exceed the depth of the
387 debris mantle for the duration of the secondary deglaciation process
388 resulting in continued and complete melting of buried-ice despite an
389 increasing debris thickness. The findings of Midgley et al. (2013) indicated
390 that sediment concentration within the moraine is low in lateral positions

391 compared to frontal positions. As a result, following complete de-icing the
392 lateral features which have a significant ice component are likely to be
393 topographically low and diffuse relative to the frontal features where the
394 total volume of sediment appears to be much larger. This is an important
395 consideration where high-Arctic polythermal glaciers are used as an
396 analogue for relict glacial landsystems in the geomorphological record.

397 *5.3. Controls on rates of down-wasting*

398 The physical properties of the insulating debris layer such as its thickness,
399 water content and thermal conductivity influence rates of moraine down-
400 wastage (Schomacker, 2008). The importance of rainwater depends on the
401 extent to which the influence of heat advection via percolation is countered
402 by evaporation from the ground surface (Sakai et al., 2004). Rainwater has
403 been shown to be important in facilitating top-melt in highly permeable
404 substrates (Reznichenko et al., 2010), at least where cool and damp
405 atmospheric conditions limit evaporation. Conversely, block-rich material
406 with high surface roughness has low thermal conductivity and can obstruct
407 the development of winter snow-cover depressing the lower limit of
408 permafrost in mountain terrain (Etzelmüller and Frauenfelder, 2009). At
409 Austre Lovénbreen, the substrate typically consists of clast-rich diamictons
410 which are overlain by gravels with a variable fine component in many places.
411 Diamictons have been associated with variable porosity values (e.g.
412 Parriaux and Nicoud, 1990; Kilfeather and van der Meer, 2008; Burki et al.,
413 2010; Worni et al., 2012). Diamicton with silt and clay components and

414 frozen horizons will lower the permeability of the debris, and serve to
415 impede heat advection by water during summer months, thus limiting ice-
416 ablation (e.g. Reznichenko et al., 2010).

417 Local topographic controls also influence air-temperature and subsequently
418 permafrost distribution (Harris et al. 2009). Strong topographic shading
419 has been reported as an influence on de-icing at other sites in Svalbard
420 (e.g. Lyså and Lønne , 2001). Given the proximity of the landform to
421 Slattofljettet (582 m), rates of moraine down-wastage in up-glacier
422 sections of the landform may be influenced. Modelling of these shading
423 effects is likely to be an interesting avenue of research in relation to
424 moraine disintegration and more generally, permafrost distribution and
425 properties in mountainous terrain.

426 A further confounding factor is snow-cover which is known to limit the
427 influence of atmospheric heat on ground temperature (Stieglitz et al.,
428 2003). Whilst in winter snow may permit higher ground temperature in
429 relation to mean air temperatures (Stieglitz et al., 2003), late lying snow is
430 likely to play an additional role limiting the susceptibility of buried-ice to
431 surface warming. Further work investigating the influence of snow cover
432 and snow-depth in relation to moraine down-wastage could elucidate how
433 significant a role it plays in reducing down-wastage.

434 *5.4. Spatial variations within the moraine system*

435 Diminishing rates of landform change from areas Z_1 to Z_3 (Fig. 3)
436 correspond with an increase in the proportion of debris relative to ice from

lateral to frontal positions (e.g. Midgley et al., 2013). Spatially variable amounts of buried-ice imply that the mode of moraine formation is not consistent across the moraine complex (e.g. Hambrey and Glasser, 2012). Lateral sections conform to the 'controlled' ice-cored model of moraine formation (e.g. Evans, 2009) where the release of material from debris-rich folia result in surface linearity and form an insulating surface layer for underlying glacier-ice. The reduced rates of observed surface lowering in the frontal sections, and the presence of surface hummocks indicate that separate glaciological and geomorphological processes are responsible for the emplacement of moraine at different locations along the lateral-frontal complex. Here, structural glaciology and the preferential entrainment of basal debris in frontal locations are likely to be important. For example, studies have investigated the development of surface hummocks ('hummocky moraine') in relation to the stacking of englacial material along thrusts planes (e.g. Hambrey et al., 1996; 1997; Bennett et al., 1998; Graham, 2002; Midgley et al., 2007). The processes described in these papers may, in part, be responsible for areas of surface hummocks on the moraine complex and lower levels of ice incorporation. It is worth noting that additional moraine forming processes such as pushing and permafrost deformation are documented to occur in ice-marginal environments in Svalbard (Etzelmüller et al., 1996; Boulton et al., 1999).

6. Summary

The evolution of an ice cored lateral-frontal moraine over an 11-year period was assessed at the high-Arctic polythermal glacier Austre Lovénbreen, Svalbard. Repeat DEMs and DEMs of difference were generated from archive and UAV-derived aerial imagery using SfM and minLOD methods. Average depth of surface lowering for the entire study area was estimated to be −1.75 ± 0.89 m. Landform evolution occurred most rapidly on lateral sections of the landform. In contrast to many other sites in Svalbard, field evidence highlights that the moraine appears to be de-icing predominately by down-wastage, affording the landform higher levels of stability. Atypical of de-icing moraines in the high-Arctic, slope and fluvial driven change appear to be less significant. There may be potential for the buried-ice to be stabilised and preserved as a palaeoglaciological archive of former Neoglacial ice dynamics. The high-resolution UAV-derived dataset serves as a benchmark for future studies monitoring geomorphological change on the lateral-frontal moraine at Austre Lovénbreen, achieving a vertical *RMSE* value of 0.048 m for independent check points. This study adds to the growing body of evidence that a combination of UAV-derived imagery, a consumer-grade digital camera and SfM methods are highly appropriate for monitoring of geomorphological change. The errors associated with DEM generation from archived conventional aerial imagery were substantially larger, partly as a result of the lower image resolution, and partly the limited availability of appropriate features to use for ground control. Such issues are common to the extraction of topographic data from archive

imagery in changing environments, and may limit the application of this approach. Nevertheless, the derived DEM was of sufficient quality to be useful for estimating the rate of de-icing over the 11-year period investigated. It is concluded that the use of SfM photogrammetry for extracting morphological data from a range of aerial imagery is appropriate for monitoring environmental change and is likely to have wider applications in other geoscientific sub-disciplines.

Acknowledgments

This research was undertaken whilst TNT was funded by a Nottingham Trent University VC bursary. Additional grants from Nottingham Trent University to NGM and from the Manchester Geographical Society to SJC made this work possible. The fieldwork benefited from the logistical support provided by Nick Cox of the UK Natural Environment Research Council (NERC) Arctic Research Station. Anya Wicikowski is thanked for assisting with field data collection. Aerial image data from the UK Natural Environment Research Council (NERC) Airborne Research and Survey Facility (ARSF) are provided courtesy of NERC via the NERC Earth Observation Data Centre (NEODC). Permission to conduct aerial survey work was obtained from the Norwegian CAA and the relevant local authorities. Dr. David Rippin is thanked for providing advice on Norwegian airspace permission applications. Additional thanks go to Marc Shallbrook for providing advice on data preparation. The manuscript was improved following helpful comments from Dr. Marek Ewertowski and one anonymous reviewer.

Fig. 1. Location map of Svalbard and the study site in relation to Austre Lovénbreen (AL). Data from Norwegian Polar Institute (2014).

Fig. 2. Locations of ground-control applied to the 2003 and 2014 topographic datasets and the independent check-points used for error analysis on the 2014 DEM. The black line indicates the extent of the 2003 SfM DEM. The orthophoto is produced from aerial image data collected in 2003 by the UK Natural Environment Research Council (NERC) Airborne Research and Survey Facility (ARSF). These data are provided courtesy of NERC via the NERC Earth Observation Data Centre (NEODC).

Fig. 3. Surface change over the western lateral-frontal moraine of Austre Lovénbreen. (A) DEM of difference for 2003–2014. The black lines are contour data (m.a.s.l.) derived from the 2014 DEM. The locations of three zones of analysis (Z_1, Z_2 and Z_3) are shown. (B) Surface change in relation to area and volume. (C) Average surface change for Z_1, Z_2 and Z_3 with the minimum level of detection (minLOD) highlighted by the dotted line.

Fig. 4. Surface evolution over the 11-year study period demonstrated by three topographic profiles. (A) The locations of the three profiles. (B) Surface change along profiles 1-3 between 2003 and 2014.

Fig. 5. Relative abundance of geomorphological features indicative of surface change across the study area.

Fig. 6. Conceptual model for the evolution of the lateral-frontal moraine under the scenarios of partial and complete de-icing.

References

Arnold N.S., Rees. W.G., Devereux, B.J. and Amable., G.S. 2006. Evaluating the potential of high-resolution airborne LiDAR data in glaciology. International Journal of Remote Sensing, 27 (6), 1233–1251. doi:10.1080/01431160500353817

Benn, D.I., Lukas, S., 2006. Younger Dryas glacial landsystems in North West Scotland: An assessment of modern analogues and palaeoclimatic implications. Quaternary Science Reviews. 25, 2390-2408. doi:10.1016/j.quascirev.2006.02.015

Bennett, G.L. & Evans, D.J.A. 2012. Glacier retreat and landform production on an overdeepened glacier foreland: the debris-charged glacial landsystem at Kvíárjökull, Iceland. Earth Surface Processes and Landforms, 37 (15), 1584-1602. doi: 10.1002/esp.3259

Bennett, M.R., Huddart, D., Hambrey, M.J. and Ghienne, J.F. 1996. Moraine Development at the High-Arctic Valley Glacier Pedersenbreen, Svalbard. *Geografiska Annaler. Series A, Physical Geography*, 78 (4), 209-222.

Bennett, M.R., Hambrey, M.J., Huddart, D. and Glasser, N.F., 1998. Glacial thrusting and moraine-mound formation in Svalbard and Britain: the example of Coire a' Cheud-chnoic (Valley of hundred hills), Torridon, Scotland. Quaternary Proceedings, 6, 17–34.

Bennett, M.R., Huddart, D., Glasser, N.F. and Hambrey, M.J. 2000. Resedimentation of debris on an ice-cored lateral moraine in the high-Arctic

549 (Kongsvegen, Svalbard). Geomorphology, 35, 21-40. doi:10.1016/S0169-
550 555X(00)00017-9

551 Boulton, G., van der Meer, J.J.M., Beets, D.J., Hart, J.K. and Ruegg, G.H.J.
552 1999. The sedimentary and structural evolution of a recent push moraine
553 complex: Holmstrombreen, Spitsbergen. Quaternary Science Reviews, 18,
554 339-371.

555 doi:10.1016/S0277-3791(98)00068-7

556 Brasington, J., Langham, J. and Rumsby B. 2003. Methodological sensitivity
557 of morphometric estimates of coarse fluvial sediment transport.
558 Geomorphology, 53 (3–4), 299–316. doi: 10.1016/S0169-555X(02)00320-
559 3

560 Burki, V., Hansen, L., Fredin, O., Andersen, T.A., Beylich, A.A., Jaboyedoff,
561 M., Larsen, E., Tønnesen, J.-F. 2010. Little Ice Age advance and retreat
562 sediment budgets for an outlet glacier in western Norway. Boreas, 39 (3)
563 (2010), 551–566. doi: 10.1111/j.1502-3885.2009.00133.x

564 Clapuyt, F., Vanacker, V., Van Oost, K. 2015. Reproducibility of uav-based
565 earth topography reconstructions based on structure-from-motion
566 algorithms. Geomorphology, In press.
567 doi:10.1016/j.geomorph.2015.05.011

568 Carrivick, J.L., Smith, M.W., Quincey, D.J. and Carver, S.J. 2013.
569 Developments in budget remote sensing for the geosciences. Geology
570 Today, 29, 138–143. doi: 10.1111/gto.12015

571 Etzelmüller, B. 2000. Quantification of thermo-erosion in pro-glacial areas
572 - examples from Svalbard. Zeitschrift für Geomorphologie, 44, 343-361.

573 Etzelmüller, B. and Frauenfelder, R. 2009. Factors Controlling The
574 Distribution of Mountain Permafrost in The Northern Hemisphere and Their
575 Influence on Sediment Transfer. Arctic, Antarctic, and Alpine Research, 41
576 (1), 48-58. DOI: 10.1657/1938-4246(08-026)[ETZELMUELLER]2.0.CO;2

577 Etzelmüller, B. and Hagen, J.O. 2005. Glacier permafrost interaction in
578 arctic and alpine environments – examples from southern Norway and
579 Svalbard. In: Harris, C. & Murton, J. (eds.). Cryospheric systems – Glaciers
580 and Permafrost. British Geol. Soc., Spec. Publ. 242, 11-27.

581 Etzelmüller, B., Hagen, J.O., Vatne, G., Ødegård, R.S., Sollid, J.L. 1996.
582 Glacier debris accumulation and sediment deformation influenced by
583 permafrost, examples from Svalbard. Ann. Glaciol., 22, 53 – 62.

584 Etzelmüller, B., Ødegård, R.S., Vatne, G., Mysterud, S., Tonning, T and
585 Sollid, J.L. 2000. Glacier characteristics and sediment transfer system of
586 Longyearbreen and Larsbreen, western Spitsbergen. Norsk Geografisk
587 Tidsskrift, 54 (4), 157-168. DOI:10.1080/002919500448530

588 Evans, D.J.A. 2009. Controlled moraines: origins, characteristics and
589 palaeoglaciological implications. Quaternary Science Reviews, 28 (3-4),
590 181-260. doi: 10.1016/j.quascirev.2008.10.024

591 Everest, J. and Bradwell, T. 2003. Buried glacier ice in southern Iceland and
592 its wider significance. Geomorphology, 52 (3-4). 347–358.
593 http://dx.doi.org/10.1016/S0169-555X(02)00277-5

594 Ewertowski M., Kasprzak L., Szuman I., Tomczyk A.M., 2012. Controlled,
595 ice-cored moraines: sediments and geomorphology. An example from
596 Ragnarbreen, Svalbard. Zeitschrift für Geomorphologie, 56 (1), 53-74. doi:
597 10.1127/0372-8854/2011/0049

598 Ewertowski. M. 2014. Recent transformations in the high-Arctic glacier
599 landsystem, Ragnarbreen, Svalbard. Geografiska Annaler: Series A
600 (Physical Geography), 96, 265-285. doi: 10.1111/geoa.12049

601 Ewertowski, M. and Tomczyk, A.M. 2015. Quantification of the ice-cored
602 moraines' short-term dynamics in the high-Arctic glaciers Ebbabreen and
603 Ragnarbreen, Petuniabukta, Svalbard. Geomorphology, 234, 211-227. doi:
604 10.1016/j.geomorph.2015.01.023

605 Friedt, J.-M., Tolle, F., Bernard, É., Griselin, M., Laffy, D and Marlin, C. 2012.
606 Assessing the relevance of digital elevation models to evaluate glacier mass
607 balance: application to Austre Lovénbreen (Spitsbergen, 79°N). Polar
608 Record, 48 (244) 2–10. DOI: 10.1017/S0032247411000465

609 Fonstad, M.A., Dietrich, J.T., Courville, B.C. and Carbonneau, P.E. 2013.
610 Topographic structure from motion: a new development in
611 photogrammetric measurements. Earth Surface Processes and Landforms,
612 20, 817-827. doi: 10.1002/esp.3366

613 Graham, D.J. 2002. Moraine–mound formation during the Younger Dryas
614 in Britain and the Neoglacial in Svalbard. PhD thesis University of Wales,
615 Aberystwyth.

616 Graham, D.J. and Hambrey, M.J. 2007. Sediments and landforms in an
617 upland glaciated-valley landsystem: Upper Ennerdale, English Lake District
618 in M.J. Hambrey, P. Christoffersen, N.F. Glasser NF and B. Hubbard (Eds),
619 Glacial Sedimentary Processes and Products, Blackwell, Oxford (2007),
620 235-256.

621 Graham, D.J. and Midgley, N.G. 2000. Moraine-mound formation by
622 englacial thrusting: the Younger Dryas moraines of Cwm Idwal, North
623 Wales. In: A.J. Maltman, B. Hubbard and M.J. Hambrey (eds.), Deformation
624 of Glacial Materials. London: Geological Society, pp. 321-336.
625 http://dx.doi.org/10.1144/GSL.SP.2000.176.01.24
626 Glasser, N.F. and Hambrey, M.J. 2003. Ice-marginal terrestrial landsystems:
627 Svalbard polythermal glaciers in D.J.A. Evans (Ed.), Glacial Landsystems,
628 Hodder Arnold, London (2003), 65–88.

629 Glasser, N.F., Coulsen, S.J., Hodkinson, I.D. and Webb, N.R. 2004.
630 Photographic evidence of the return period of a Svalbard surge-type glacier:
631 a tributary of Pedersenbreen, Kongsfjord. Journal of Glaciology, 50 (169),
632 307-308.

633 Hambrey, M.J., Dowdeswell, J.A., Murray, T., Porter, P.R., 1996. Thrusting
634 and debris entrainment in a surging glacier: Bakaninbreen, Svalbard.
635 Annals of Glaciology, 22, 241-248.

636 Hambrey, M.J., Huddart, D., Bennett, M.R. and Glasser, N.F. 1997. Genesis
637 of "hummocky moraines" by thrusting in glacier ice: evidence from
638 Svalbard and Britain. Journal of the Geological Society, London. 154, 623-
639 632. doi: 10.1144/gsjgs.154.4.0623

640 Hambrey, M.J., Murrary, T., Glasser, N.F., Hubbard, A., Hubbard, B., Stuart,
641 G., Hansen, S. and Kohler, J. 2005. Structure and changing dynamics of a
642 polythermal valley glacier on a centennial time-scale: midre Lovénbreen,
643 Svalbard. Journal of Geophysical Research, Earth Surface, p. F010006.

644 Hambrey, M.J. and Glasser, N.F. 2012. Discriminating glacier thermal and
645 dynamic regimes in the sedimentary record, Sedimentary Geology, 251–
646 252, 1–33. doi:10.1016/j.sedgeo.2012.01.008

647 Hansen, S. 2003. From surge-type to non-surge type glacier behaviour:
648 Midre Lovénbreen, Svalbard. Annals of Glaciology, 36, 97–102.

649 Harris, C., Arenson, L.U., Christiansen, H.H., Etzelmüller, B., Fraunfelder,
650 R., Gruber., Haeberli, W., Hauck, C., Hölzle, M., Humlum, O., Isaksen, K.
651 Kääb, A., Kern-Lütschg, M.A., Lehning, M., Matsuoka, N., Murton, J.B.,
652 Nötzlie, J., Philips, M., Ross, N., Seppäläl, M., Springman, S.M. and Mühll,
653 D.V. 2009. Permafrost and climate in Europe: Monitoring and modelling
654 thermal, geomorphological and geotechnical responses. 92 (3-4), 117-171.
655 doi: 10.1016/j.earscirev.2008.12.002

656 Isachsen, G. 1912. Exploration du Nord-Ouest du Spitsberg entreprise sous
657 les auspices de S.A.S. le Prince de Monaco par la Mission Isachsen.
658 Fascicule XL. Imprimerie de Monaco.

659 Irvine-Fynn, T.D.L., Barrand, N.E., Porter, P.R., Hodson, A.J. and Murray,
660 T. 2011. Recent High-Arctic glacial sediment redistribution: a process
661 perspective using airborne lidar. Geomorphology, 125 (1), 27–39.
662 doi:10.1016/j.geomorph.2010.08.012

663 Ingólfsson, Ó and Lokrantz, H. 2003. Massive ground ice body of glacial
664 origin at Yugorski Peninsula, arctic Russia. Permafrost and Periglacial
665 Processes, 14 (3), 199–215. doi: 10.1002/ppp.455

666 James, M. R. and Robson, S. 2012. Straightforward reconstruction of 3D
667 surfaces and topography with a camera: Accuracy and geoscience
668 application, J. Geophys. Res., 117, F03017, doi: 10.1029/2011JF002289

669 Jiskoot, H., Murray, T. and Boyle, P.J. 2000. Controls on the distribution of
670 surge-type glaciers in Svalbard. Journal of Glaciology, 46 (154) 412–422.
671 doi: 10.3189/172756500781833115

672 King, E.C., Smith, A.M., Murray, T. and Stuart, G.W. 2008. Glacier-bed
673 characteristics of midtre Lovénbreen, Svalbard, from high ‐ resolution
674 seismic and radar surveying, J. Glaciol., 54, 145 – 156,
675 doi:10.3189/002214308784409099.

676 Kilfeather , A.A. and van der Meer, J.J.M. 2008. Pore size, shape and
677 connectivity in tills and their relationship to deformation processes.
678 Quaternary Science Reviews, 27 (3–4) 250–266. doi:
679 10.1016/j.quascirev.2006.12.015

680 Kirkbride, M.P. and Winkler, S. 2012. Correlation of Late Quaternary
681 moraines: impact of climate variability, glacier response, and chronological
682 resolution. Quaternary Science Reviews, 46, 1-29.
683 doi:10.1016/j.quascirev.2012.04.002

684 Kjær, K.H and Krüger, J. 2001. The final phase of dead-ice moraine
685 development: processes and sediment architecture, Kötlujökull, Iceland.
686 Sedimentology, 48 (5), 935-952. doi: 10.1046/j.1365-3091.2001.00402.x

687 Krüger, J. and Kjær, K.H. 2000. De-icing progression of ice-cored moraines
688 in a humid, sub-polar climate, Kotlujökull, Iceland. The Holocene, 48, 935–
689 952. doi: 10.1191/09596830094980

690 Krüger, J., Kjær, K.H., Schomacker, A. 2010. Dead-Ice Environments: A
691 Landsystems Model for a Debris-Charged, Stagnant Lowland Glacier Margin,
692 Kötlujökull. Developments in Quaternary Sciences. 13, 105-126.
693 doi:10.1016/S1571-0866(09)01307-4

694 Lønne, I. and Lysså, A. 2005. Deglaciation dynamics following the Little Ice
695 Age on Svalbard: Implications for shaping of landscapes at high latitudes.
696 Geomorphology 72, 300–319. doi:10.1016/j.geomorph.2005.06.003

697 Lucieer, A., de Jong, S.M, and Turner, D. 2013. Mapping landslide
698 displacements using Structure from Motion (SfM) and image correlation of
699 multi-temporal UAV photography. Progress in Physical Geography, 38 (1),
700 97-116. doi: 10.1177/0309133313515293

Lukas, S., Nicholson, L.I., Ross, F.H and Humlum, O. 2005 Formation, meltout processes and landscape alteration of High-Arctic ice-cored moraines—examples from Nordenskiold Land, Central Spitsbergen. Polar Geography, 29 (3), 157–187. doi: 10.1080/789610198

Lysså, A. and Lønne. I. 2001. Moraine development at a small High-Arctic valley glacier: Rieperbreen, Svalbard. Journal of Quaternary Science, 16 (6), 519–529. doi: 10.1002/jqs.613

Midgley, N.G., Glasser, N.F. and Hambrey, M.J. 2007. Sedimentology, structural characteristics and morphology of a Neoglacial high-Arctic moraine–mound complex: Midre Lovénbreen, Svalbard. in: M.J. Hambrey, P. Christoffersen, N.F. Glasser, B. Hubbard (Eds.), Glacial Sedimentary Processes and Products, International Associated of Sedimentologists, Special Publication, 39 (2007), 11–23.

Midgley, N.G., Cook, S.J., Graham, D.J. and Tonkin, T.N. 2013. Origin, evolution and dynamic context of a Neoglacial lateral–frontal moraine at Austre Lovénbreen, Svalbard. Geomorphology, 198, 96-106. doi:10.1016/j.geomorph.2013.05.017

Murton J.B., Whiteman, C.A., Waller, R.I., Pollard, W.H., Clark, I.D. and Dallimore, S.R. 2005. Basal ice facies and supraglacial melt-out till of the Laurentide Ice Sheet, Tuktoyaktuk Coastlands, western Arctic Canada. Quaternary Science Reviews. 24 (5-6), 681-708. doi:10.1016/j.quascirev.2004.06.008

723 Norwegian Polar Institute 2014. Kartdata Svalbard 1:100 000 (S100
724 Kartdata). Tromsø, Norway: Norwegian Polar Institute. Available at:
725 https://data.npolar.no/dataset/645336c7-adfe-4d5a-978d-9426fe788ee3

726 Parriaux, A. and Nicoud. G.F. 1990. Hydrological behaviour of glacial
727 deposits in mountainous areas, in: L. Molnár (Ed.), Hydrology of
728 Mountainous Areas, International Association of Hydrological Sciences,
729 Publication, 190 (1990), 291–311.

730 Reznichenko, N., Davies, T., Shulmeister, J. and McSaveney, M. 2010.
731 Effects of debris on ice surface melting rates: an experimental study.
732 Journal of Glaciology, 56 (197), 384-394. doi:
733 10.3189/002214310792447725

734 Rippin, D.M., Pomfret, A. and King, N. 2015. High resolution mapping of
735 supra-glacial drainage pathways reveals link between micro-channel
736 drainage density, surface roughness and surface reflectance. Earth Surface
737 Processes and Landforms. Early view. doi: 10.1002/esp.3719

738 Ryan, J.C., Hubbard, A.L., Box, J.E., Todd, J., Christoffersen, P., Carr, J.R.,
739 Holt, T.O., Snooke, N. 2015. UAV photogrammetry and structure from
740 motion to assess calving dynamics at Store Glacier, a large outlet draining
741 the Greenland ice sheet. The Cryosphere, 9, 1-11. doi:10.5194/tc-9-1-
742 2015

743 Sakai, A., Fujita, K. and Kubota. J. 2004. Evaporation and percolation effect
744 on melting at debris-covered Lirung Glacier, Nepal Himalayas, 1996.
745 Bulletin of Glaciological Research, 21, 9–16.

746 Saintenoy, A., Friedt, J.-M., Booth, A.D., Tolle, F., Bernard, E., Laffly, D.,
747 Marlin, C. and Griselin, M. 2012. Deriving ice thickness, glacier volume and
748 bedrock morphology of Austre Lovénbreen (Svalbard) using GPR. Near
749 Surface Geophysics, 11 (2), 253–26. doi: 10.3997/1873-0604.2012040

750 Schäfer, J.M., Heinrich, B., Denton, G.H., Ivy-Ochs, S., Marchant, D.R.,
751 Schlüchter, C. and Rainer, W. 2000. The oldest ice on Earth in Beacon
752 Valley, Antarctica: new evidence from surface exposure dating. Earth and
753 Planetary Science Letters. 179 (1), 91-99.

754 Schiefer, E. and Gilbert, R. 2007. Reconstructing morphometric change in
755 a proglacial landscape using historical aerial photography and automated
756 DEM generation. Geomorphology, 88 (1-2), 167-178.
757 doi:10.1016/j.geomorph.2006.11.003

758 Schomacker, A. 2008. What controls dead-ice melting under different
759 climate conditions? A discussion. Earth-Science Reviews, 90 (3-4), 103-113.

760 Schomacker, A. and Kjær, K.H. 2007. Origin and de-icing of multiple
761 generations of ice-cored moraines at Brúarjökull, Iceland. 36 (4), 411-425.

762 Schomacker, A. and Kjær, K.H. 2008. Quantification of dead-ice melting in
763 ice-cored moraines at the high-Arctic glacier Holmstrombreen, Svalbard.
764 Boreas, 37, 211–225. doi: 10.1111/j.1502–3885.2007.00014.x.

765 Smith, M.W. and Vericat, D. 2015. From experimental plots to experimental
766 landscapes: topography, erosion and deposition in sub-humid badlands

767 from Structure-from-Motion photogrammetry. Earth Surface Processes and
768 Landforms. Early View. doi: 10.1002/esp.3747

769 Staines, K.E., Carrivick, J.L., Tweed, F.S., Evans, A.J., Russell, A.J.,
770 Jóhannesson, T. and Roberts, M. 2015. A multi-dimensional analysis of
771 proglacial landscape change at Sólheimajökull, southern Iceland. Earth
772 Surface Processes and Landforms. Available online from 14/11/2014. doi:
773 10.1002/esp.3662

774 Stieglitz, M., Déry, S.J., Romanovsky, V.E., Osterkamp, T.E. 2003. The
775 role of snow cover in the warming of arctic permafrost. Geophysical Reserch
776 Letters, 30 (13), 1721. doi:10.1029/2003GL017337

777 Sugden, D.E., Marchant, D.R., Potter Jr. N., Souchez, R.A., Denton, G.H.,
778 Swischer III, C.C. and Tison, J.-L. 1995. Preservation of Miocene glacier ice
779 in East Antarctica. Nature, 376, 412–414. doi:10.1038/376412a0

780 Tonkin, T.N., Midgley, N.G., Graham, D.J. and Labadz, J.C. 2014. The
781 potential of small unmanned aircraft systems and structure-from-motion
782 for topographic surveys: A test of emerging integrated approaches at Cwm
783 Idwal, North Wales. Geomorphology, 226, 35-43. doi:
784 10.1016/j.geomorph.2014.07.021

785 Waller, R.I., Murton, J.B. and Kristensen, L. 2012. Glacier-permafrost
786 interactions: Processes, products and glaciological implications.
787 Sedimentary Geology, 255, 1-28. doi: /10.1016/j.sedgeo.2012.02.005

788 Wheaton, J.M., Brasington, J., Darby, S.E. and Sear, D.A. 2010. Accounting
789 for uncertainty in DEMs from repeat topographic surveys: improved
790 sediment budgets. Earth Surface Processes and Landforms, 35 (2), 136-
791 156. doi: 10.1002/esp.1886

792 Worni, R., Stoffel, M., Huggel, C., Volz, C., Casteller, A. and Luckman, B.
793 2012. Analysis and dynamic modeling of a moraine failure and glacier lake
794 outburst flood at Ventisquero Negro, Patagonian Andes (Argentina). Journal
795 of Hydrology, 444–445, 134–145. doi:10.1016/j.jhydrol.2012.04.013

796 Westoby, M., Brasington J, Glasser, N.F., Hambrey, M.J. and Reyonds, M.J.
797 2012. Structure-from-Motion photogrammetry: a low-cost, effective tool
798 for geoscience applications. Geomorphology, 179, 300-314.
799 doi:10.1016/j.geomorph.2012.08.021

800

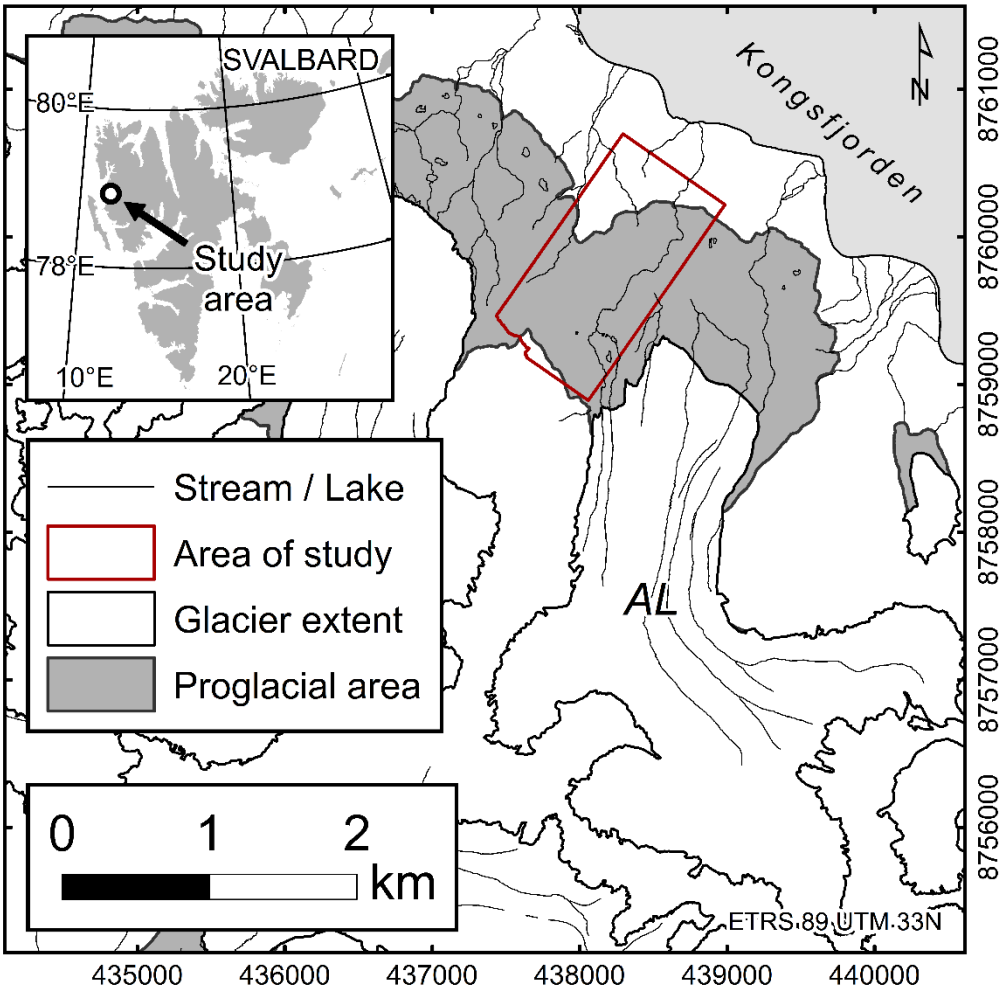
SVALBARD
80°E
78°E
Study
area
10°E
20°E
Kongsfjorden
N
AL
Stream / Lake
Area of study
Glacier extent
Proglacial area
0
1
2
km
ETRS 89 UTM 33N
435000
436000
437000
438000
439000
440000
8761000
8760000
8759000
8758000
8757000
8756000

801

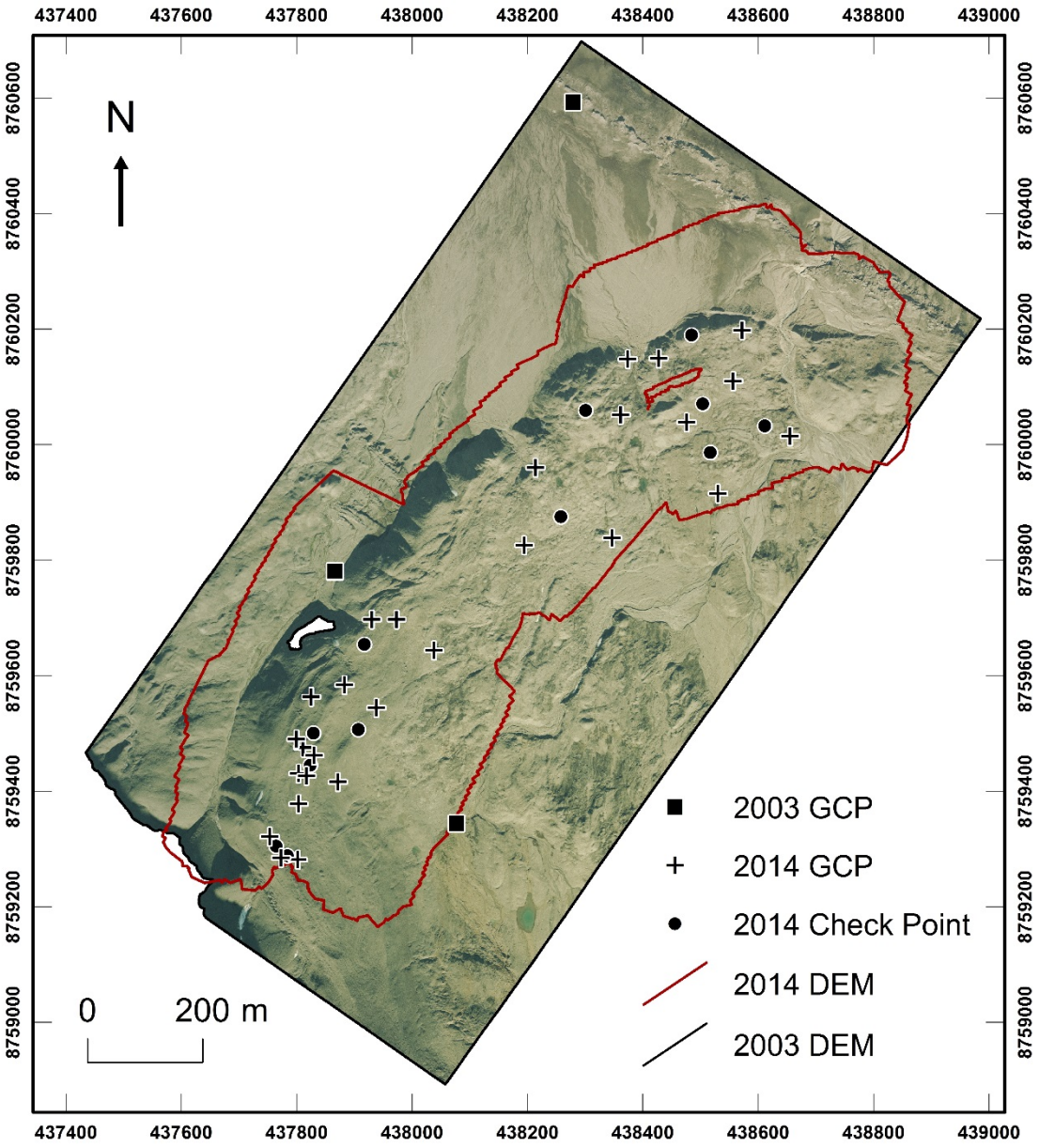
437400
437600
437800
438000
438200
438400
438600
438800
439000
8760600
8760400
8760200
8760000
8759800
8759600
8759400
8759200
8759000
N
0
200 m
2003 GCP
2014 GCP
2014 Check Point
2014 DEM
2003 DEM

802

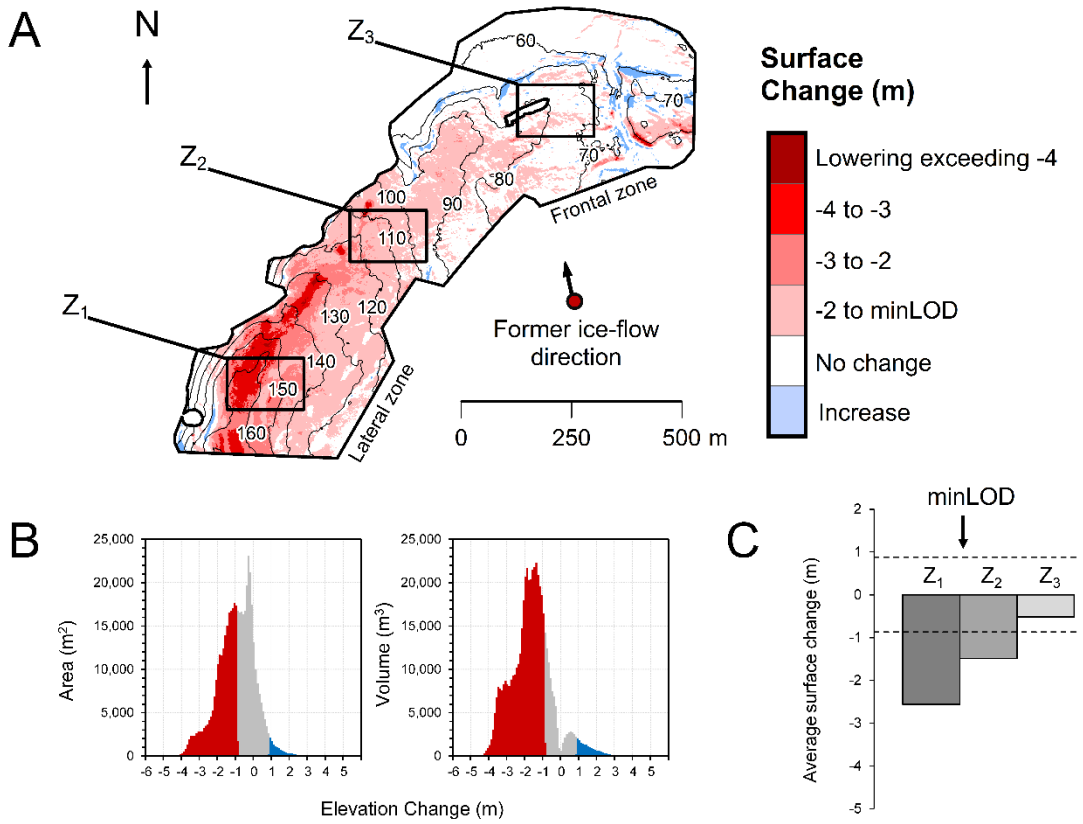
A
N
Z3
Z2
Z1
60
70
70
80
90
100
110
120
130
140
150
160
Frontal zone
Lateral zone
Former ice-flow direction
0
250
500 m
Surface Change (m)
Lowering exceeding -4
-4 to -3
-3 to -2
-2 to minLOD
No change
Increase
B
Area (m²)
Volume (m³)
Elevation Change (m)
C
minLOD
Z1
Z2
Z3
Average surface change (m)

803

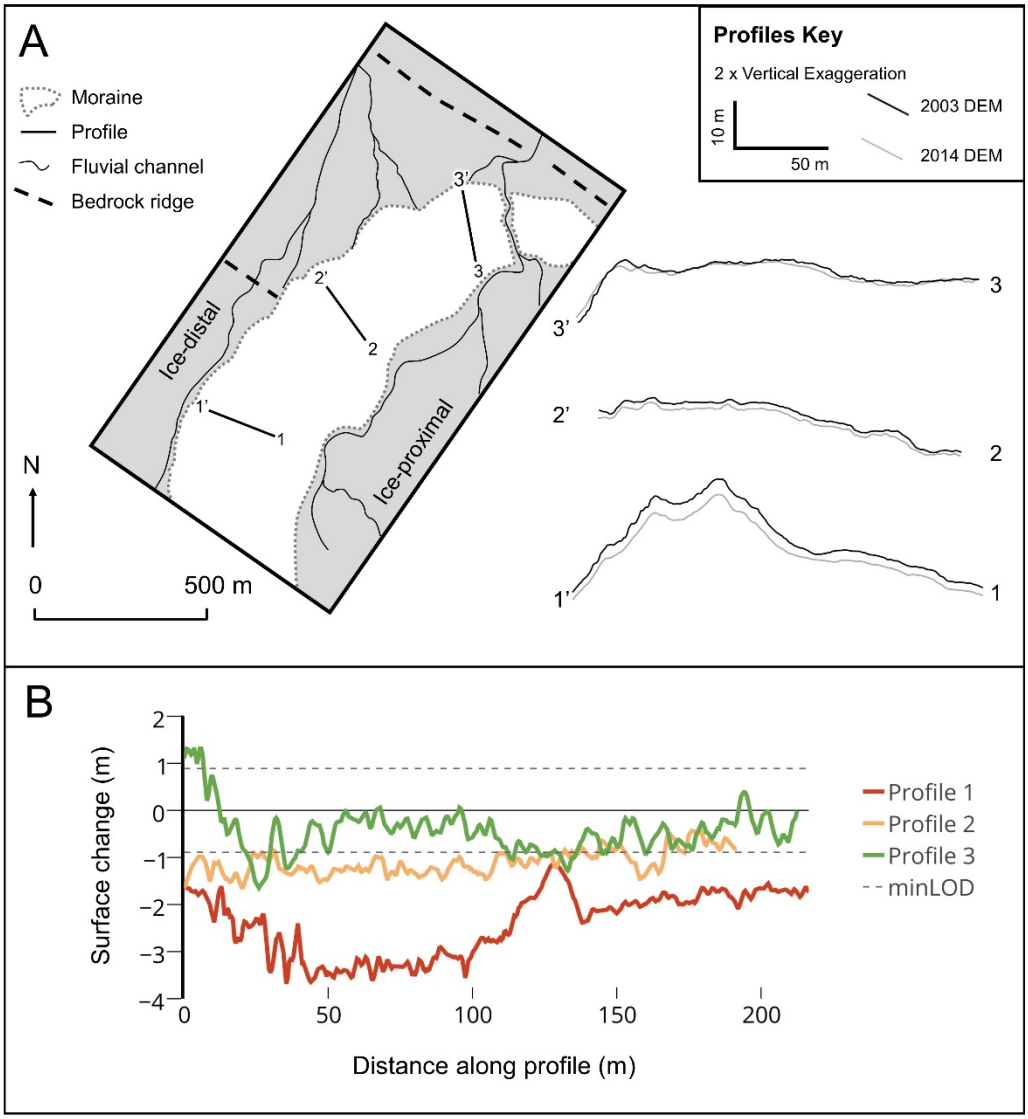
A
Moraine
Profile
Fluvial channel
Bedrock ridge
Profiles Key
2 x Vertical Exaggeration
10 m
50 m
2003 DEM
2014 DEM
Ice-distal
Ice-proximal
1'
1
2'
2
3'
3
N
0
500 m
B
Surface change (m)
Distance along profile (m)
Profile 1
Profile 2
Profile 3
minLOD

804

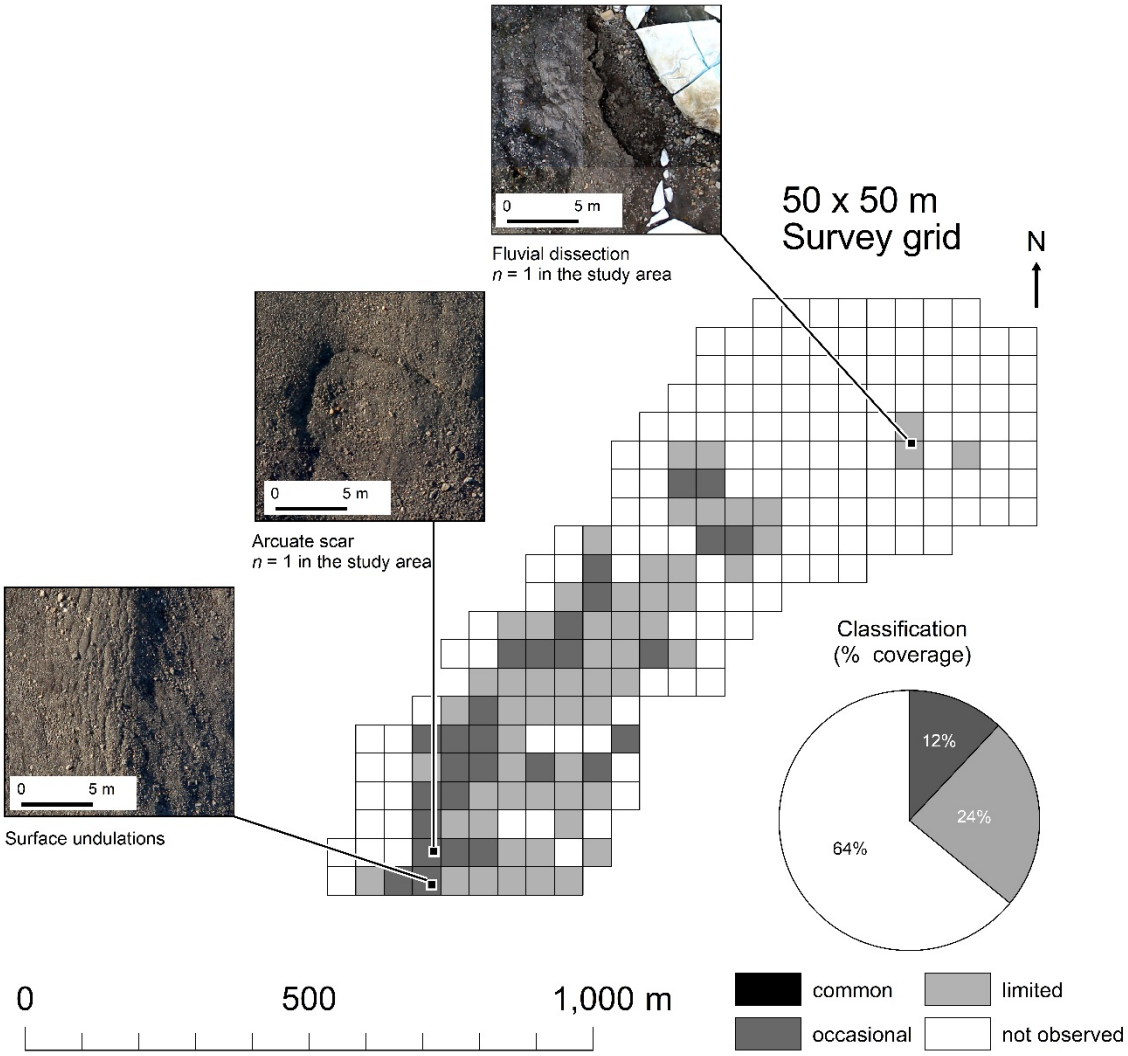
0 5 m
Fluvial dissection
n = 1 in the study area
50 x 50 m
Survey grid
N
0 5 m
Arcuate scar
n = 1 in the study area
0 5 m
Surface undulations
Classification
(% coverage)
12%
24%
64%
0
500
1,000 m
common
limited
occasional
not observed

805

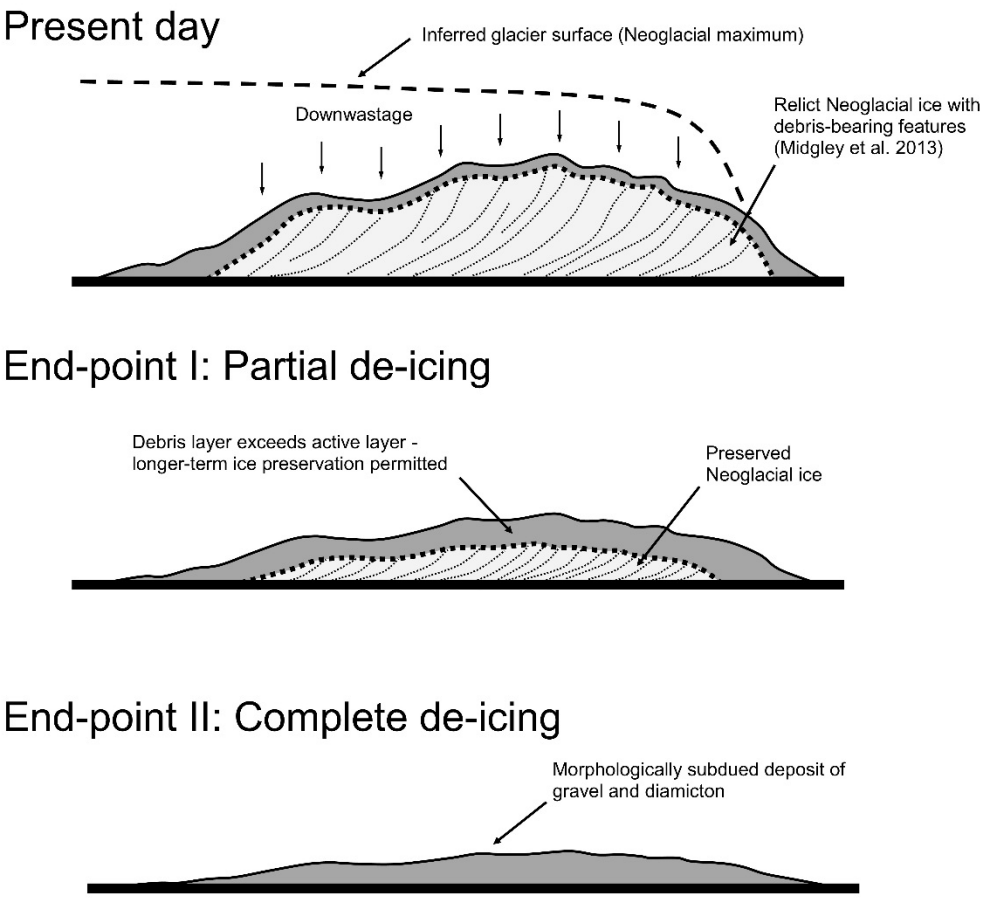
Present day
Inferred glacier surface (Neoglacial maximum)
Downwastage
Relict Neoglacial ice with debris-bearing features (Midgley et al. 2013)
End-point I: Partial de-icing
Debris layer exceeds active layer - longer-term ice preservation permitted
Preserved Neoglacial ice
End-point II: Complete de-icing
Morphologically subdued deposit of gravel and diamicton

806